ELSEVIER

Journal of Organometallic Chemistry 558 (1998) 51–60

Journal of Organometallic Chemistry

Gas-phase reactions of Tc^+, Re^+, Mo^+ and Cu^+ with alkenes

John K. Gibson *

Chemical and Analytical Sciences Division, Oak Ridge National Laboratory, Oak Ridge, TN 37831-6375, USA

Received 25 July 1997; received in revised form 16 December 1997

Abstract

Organometallic complex ions, denoted as M^+–L, where M = Tc, Re, Mo or Cu and $L = C_cH_h$, were produced by reacting laser-ablated M^+ with alkenes (R = ethene, C_2H_4; propene, C_3H_6; *cis*-2-butene, C_4H_8; cyclohexene, C_6H_{10} and 1,5-cyclooctadiene, C_8H_{12}). The compositions and abundances of the M^+–L were determined by time-of-flight mass spectrometry. A primary goal was to elucidate gas-phase organotechnetium chemistry and differentiate the behaviors of Re^+ and Mo^+ from that of Tc^+. The ion pairs, $Tc^+ + Re^+$ and $Tc^+ + Mo^+$, were coablated to provide direct comparisons of reactivities; these M^+ were ablated from solid MO_x in a copper matrix, which generated Cu^+, whose reactivity was also evaluated. For Tc^+, Re^+ and Mo^+, H_2-loss from the alkene was the primary reaction channel, and the M^+–L yields and extent of multiple H_2-loss (i.e. the reactivity) generally paralleled the size of R. Primary products were: M^+–C_2H_2 [$R = C_2H_4$]; M^+–C_3H_4 [$R = C_3H_6$]; M^+–C_4H_6 and M^+–C_4H_4 [$R = C_4H_8$]; M^+–C_6H_6 and M^+–$\{C_6H_6\}_2$ [$R = C_6H_{10}$] and M^+–C_8H_8 and M^+–C_8H_6 [$R = C_8H_{12}$]. For cycloalkenes, C–C bond cleavage also occurred, e.g. $M^+ + C_8H_{12} \rightarrow M^+\text{–}C_6H_6 + C_2H_6$. The reactivity of Re^+ was moderately greater than that of Tc^+; thus for $R = C_6H_{10}$, the yield of Tc^+–C_6H_6 and Re^+–C_6H_6 were comparable but Tc^+–C_6H_4 was minor relative to Re^+–C_6H_4. Less coherent distinctions were observed between Tc^+ and Mo^+, although Tc^+ was apparently slightly more reactive. Where ablated Mo^+ were adequately abundant to measure Mo^+–L products, a greater reactivity, compared with naked M^+, was indicated; for $R = C_6H_{10}$ the product yields were: $Tc^+\text{–}C_6H_6/Tc^+ \approx 5\%$ and $TcO^+\text{–}C_6H_6/TcO^+ \approx 40\%$. The especially facile reaction, $Tc_2^+ + C_4H_8 \rightarrow Tc_2^+\text{–}C_4H_h + [(8-h)/2]H_2$ ($h = 6$ or 4), indicated greater reactivity for Tc_2^+ compared with Tc^+. ‘Closed-shell’ ($d^{10}s^0$) Cu^+ was relatively inert, generally producing primarily the adduct, Cu^+–R (condensation was insignificant for other M^+). However, Cu^+ distinctively produced abundant Cu^+–C_4H_6 (butadiene) from C_6H_{10} and C_8H_{12}. The observed gas-phase organometallic chemistries of Cu^+ and Mo^+ are consistent with previous results by other techniques and with other organic substrates, and the reactivities of Tc^+ and Re^+ are in accord with general predictions. © 1998 Elsevier Science S.A. All rights reserved.

Keywords: Technetium; Rhenium; Molybdenum; Copper; Gas phase reactions; Mass spectrometry; Alkenes; Olefins

1. Introduction

The techniques of gas–phase organometallic chemistry have been applied to most d-block transition elements with the greatest emphasis on the ubiquitous first-row transition element ions, M^+ [1]. Results for some of the more prevalent and reactive second- and third-row M^+ have often revealed behavior not predicted from that of their lighter congeners. For example, Cr^+ is essentially inert under conditions where Mo^+ is highly reactive [2]. The unanticipated reactivity of Cu^+ [3] is another example of the incertitudes in predicting gas-phase M^+ chemistry. Particularly neglected by experimentalists have been Re^+ and especially Tc^+, owing to scarcity, and for Tc^+, owing to radioactivity; the potential for radioactive contamination is particularly problematic in gas-phase studies.

The condensed phase organometallic chemistries of both Tc [4–6] and Re [7–9] have received increased attention in the past several years due largely to widespread medical radiodiagnostic applications of short-

---

* Tel.: +1 423 5764291; fax: +1 423 5744987; e-mail: jkg@ornl.gov

PII S0022-328X(98)00400-8

Table 1
M^0 and M^+ electronic configurations and energetics[a]

	Cu	Mo	Tc	Re
Ionization energies				
$M^0 \rightarrow M^+$	7.72	7.10	7.28	7.87
$M^+ \rightarrow M^{2+}$	20.3	16.2	15.2	(16.6)
M^0 ground configurations	$3d^{10}4s$	$4d^5 5s$	$4d^5 5s^2$	$5d^5 6s^2$
M^+ configurations				
Ground	^1S $3d^{10}$	^6S $4d^5$	^7S $4d^5 5s$	^7S $5d^5 6s$
1st Excited[b]	^3D $3d^9 4s$ {2.72}	^6D $4d^4 5s$ {1.46}	^5D $4d^6$ {0.43}	^5D $5d^4 6s^2$ {1.71}
2nd Excited[b]	^1D $3d^9 4s$ {3.26}	^4G $4d^5$ {1.88}	^5S $4d^5 5s$ {1.56}	^5S $5d^5 6s$ {2.14}

[a] From [21], energies are in eV.

[b] Energy above the ground state in brackets (for lowest energy *J*-value of specified term).

lived (< 1 day half-life) γ-emitting ^{99m}Tc and potential radiotheraputic applications of β-emitting ^{188}Re [10]. In addition, ^{99}Tc is an abundant and long-lived radioactive fission product (β-decay, ca. 10^5 years half-life) whose environmental, including organometallic, chemistry should be further elucidated. Although homologous Tc and Re are chemically quite similar, significant distinctions have been noted, including a greater propensity for Re towards higher oxidation states [11]. Differences between the inorganic and organometallic chemistries of Tc and Re may be partly attributable to relativistic effects on the electron energetics and geometries for Re [12]. A primary goal of the present study of activation of alkenes by Tc^+ and Re^+ was to provide a direct comparison of their fundamental behaviors under conditions uncomplicated by solvent and other condensed phase effects. In contrast to condensed phase Tc/Re chemistry where stable high-valence state compounds are dominant, low-valence species such as M^+–arene are readily accessible under low-pressure gas-phase conditions.

Both the gas-phase [1] and condensed phase organometallic chemistries of Cu [13,14] and Mo [15,16] have been more extensively addressed than for Tc and Re; Cu^+ and Mo^+ were included as secondary reagents in the present work. The Cu^+ was an incidental by-product of the (copper matrix) target which provided in situ representation of quasi-inert behavior. Like homologous W^+ [17], Mo^+ is among the most reactive transition metal ions; Mo^+ is also of interest in comparison with Tc^+, as radioactive ^{99}Mo is the source for ^{99m}Tc.

The technique employed here is a variant of the laser ablation molecular beam (LAMB) method described by Sato [18]; the present technique is more specifically designated as laser ablation with prompt reaction and detection (LA/PRD). Essentially, nascent laser-ablated metal ions, M^+, collide with a gaseous reagent, R, and produce complex ion products, M^+–L: $\mathbf{M^+ + R \rightarrow M^+ – L + R'}$; the positive ions are measured by time-of-flight mass spectrometry (TOF-MS). The notation M^+–L is intended to convey only the aggregate composition of the product ions since their structures, bonding and charge distribution cannot be ascertained from the measurements performed. When R is an alkene, C_cH_h, typically a primary reaction channel is dehydrogenation—$L = C_cH_{h-2e}$ and $R' = eH_2$ ($e \geq 1$); condensation (L = R) and/or C–C bond activation ($L = C_xH_y$) may also constitute significant pathways. If polynuclear ions such as MO_x^+ or M_n^+ are ablated in sufficient abundance their reactivities can also be evaluated. By simultaneously ablating two or more M^+ from a multicomponent target and determining all M^+–L by TOF-MS, it is possible to compare M^+ reactivities.

A potential complication is the possibility of excited state M^{+*}, which may exhibit disparate chemistry from ground state M^+ [19]. Although nascent laser-ablated M^+ may be in an excited state, previous studies of reactions of most (11) of the lanthanide ions, Ln^+, and four actinide ions, Th^+, U^+, Np^+ and Pu^+ [20], demonstrated that coherent ground state M^+ behavior was manifested using the LA/PRD conditions employed in the present study; specifically it was concluded that most ablated Ln^+ possessed internal energies of $\lesssim 0.3$ eV. In contrast to Ln^+, which may exhibit several low-lying chemically active states, the situation is more lucid for the d-block M^+ studied here. As seen from the M^+ energetics in Table 1, the only low-energy (< 1 eV) excited configuration is $4d^6$ (^5D) Tc^{+*} at 0.46 eV above ground; since this particular excitation removes the unpaired 5s electron from ground $4d^5 5s$ (^7S) Tc^+ to fill a 4d orbital, greater chemical activity of such Tc^{+*} is generally not expected, as substantiated by the results discussed below. The primary advantage of the LA/PRD approach compared with other techniques such as FTICR-MS is the relative compactness and simplicity of the instrumentation, which has allowed enclosure of the ablation region in a radioactive-containment glovebox. In summary, although the LA/PRD results are more qualitative than those derived using more sophisticated techniques which employ FTICR-MS or guided ion beams, they can provide indications of the relative reactivities of radioactive metal ions which may not otherwise be studied.

2. Experimental

As the laser ablation mass spectrometer and its application to investigating gas-phase organometallic chemistry by LA/PRD have been described in detail elsewhere [20,22] the present description is primarily an overview. A recent modification was the enclosure of the ablation region in a glovebox designed to contain radioactive materials—the laser beam enters the glovebox through a quartz window. A XeCl (308 nm) excimer laser was focused to a ca. 0.5 mm^2 spot on a solid target. The incident energy of ca. 3 mJ pulse^{-1} corresponds to a nominal irradiance of ca. 4×10^7 W cm^{-2} (pulse duration ca. 15 ns). The reactant gas (R) was injected into the path of ablated M^+ and MO^+; unreacted M^+/MO^+ and product $M^+–L/MO^+–L$ were pulsed into a reflectron time-of-flight mass spectrometer after a delay, t_d, following the laser pulse. Typically t_d was 35 μs but was increased to 45 μs or 60 μs for a few specified experiments. Ablated ions traveled ca. 3 cm from the target to the point of injection into the flight tube; thus using $t_d = 35$ μs probed ions with a velocity of ca. 1 km s^{-1}, which corresponds to a kinetic energy ($KE_I = \{1/2\}m_I v_I^2$) of ca. 0.5 eV for ca. 100 Da ions such as Tc^+ and Mo^+, and ca. 1 eV for ca. 200 Da ions such as Re^+. The center-of-mass kinetic energy (KE_{CM}) internally dissipated in the collision of the projectile M^+ (mass m_M) with quasi-stationary R (mass m_R) is approximate as [23]: $KE_{CM} \approx \{m_R/(m_M + m_R)\}KE_I$. In the present work, KE_{CM}/KE_I ranged from ca. 0.1 (for $Re^+ + C_2H_4$) to 0.6 (for $Cu^+ + C_8H_{12}$).

The ablation targets were prepared by mixing powders of two metal oxides with an excess of Cu^0 (metal) and compressing the dispersion into a 3-mm diameter pellet. Due to the radioactivity of ^{99}Tc, target fabrication was performed in a radioactive containment glovebox. The ^{99}Tc (ORNL Isotopes Department) was nominally Tc metal but vaporization studies [11] indicated an oxide material, TcO_x—in assigning the target compositions, a stoichiometry of TcO_2 was assumed. The 99.999% Cu^0, 99.95% ReO_2 and 99% MoO_3 powders were commercial products with natural isotopic abundances: ^{nat}Cu = 69% ^{63}Cu, 31% ^{65}Cu; ^{nat}Mo = 15% ^{92}Mo, 9% ^{94}Mo, 15% ^{95}Mo, 17% ^{96}Mo, 10% ^{97}Mo, 24% ^{98}Mo, 10% ^{100}Mo and ^{nat}Re = 37% ^{185}Re, 63% ^{187}Re. Two 30 mg targets were prepared with the following aggregate compositions, expressed in mol% of total transition metal content: ‘Cu–Tc–Re’ = 91% ^{nat}Cu + 3.4% ^{99}Tc + 5.4% ^{nat}Re and ‘Cu–Mo–Tc’ = 91% ^{nat}Cu + 3.2% ^{nat}Mo + 6.1% ^{99}Tc. These targets were somewhat inhomogeneous on the scale of the ablation spot and were repositioned in situ until practical yields of both ions, $Tc^+ + Re^+$ or $Tc^+ + Mo^+$, were obtained. Although several thousand laser shots were accumulated on individual spots, no significant crater formation was apparent by visual inspection. The alkene reactants were commercial gases and liquids: 99.99% ethene, C_2H_4; 99% propene, C_3H_6; > 95% *cis*-2-butene, C_4H_8 (typical purity ca. 99%; primary impurity = *trans*-2-butene); 99% cyclohexene, *c*-C_6H_{10} and 99% 1,5-cyclooctadiene, *c*-C_8H_{12}. These reagents were bled into the ablation chamber, within 1 cm of the target. The base pressure in the flight tube was 10^{-7} mbar and increased to 10^{-6} mbar upon admission of the reactant gas; the indeterminate reactant pressure in the reaction zone must have been much greater (e.g. $\geq 10^{-4}$ mbar).

3. Results and discussion

The results generally illuminate the gas-phase organometallic chemistry of Tc^+ and its relationship to the behaviors of Re^+, Mo^+ and Cu^+. The comparative $Tc^+–Re^+$ results are of particular interest given their similar electronic configurations (d^5s) and condensed phase chemistries. It was generally more difficult to obtain quantitative results for $Tc^+–Mo^+$ due to insufficient yields of polyisotopic $^{nat}Mo^+$ and obfuscation of $^{nat}Mo^+–L$ by isobaric $^{99}Tc^+–L$ products. The relatively languid chemistry of Cu^+ reflected the chemically passive character of the filled d^{10} sub-shell and the chemistry of Cu^+ provided a useful contrast to $Tc^+/Re^+/Mo^+$, which are all rather reactive.

Several molecular ions were directly ablated, including the metal dimers, Tc_2^+, Re_2^+, Cu_2^+, $TcRe^+$, $TcCu^+$ and $ReCu^+$ at < 1% of the intensity of the M^+ constituent(s). The oxide ions, MO^+ and MO_2^+ were evident for Tc, Re and Mo (no CuO_x^+ were detected). Although the absolute yields of the $MO_{1,2}^+$ were variable, the following comparative yields were consistent (abundances normalized to M^+ intensities; inequality indicates a difference at least a factor of 2 ×):

$TcO^+ \approx ReO^+$ $\quad$ $TcO^+ < MoO^+$

$TcO_2^+ < ReO_2^+$ $\quad$ $TcO_2^+ < MoO_2^+$

The greater propensity for Re to form the pentavalent dioxide ion compared with Tc concurs with the high-temperature behavior of these elements [11]. The MO^+ yields were typically in the range of 1–10% of M^+, and the MO_2^+ yield could be up to 2% of M^+. In addition, $Tc_2^{I/II}O^+$ and $Tc_2^{II/III}O_2^+$ were occasionally identified as minor (< 1%) constituents.

Some peaks in mass spectra were assigned to free hydrocarbon fragment ions. A conspicuous example was $C_6H_9^+$ from C_6H_{10}. The yield of this H^--loss fragment was ca. ten times that of any other $C_cH_h^+$, in contrast to the 70 eV electron impact mass spectrum of c-C_6H_{10} [24] where the primary ion is $C_5H_7^+$ and H^--loss is minor. The dominant H^--loss channel here can be attributed to chemical ionization which produces strongly bonded CuH [25]:

$$Cu^+ + c\text{-}C_6H_{10} \rightarrow CuH + c\text{-}C_6H_9^+,$$

$$\Delta_r H \approx 12 \text{ kJ mol}^{-1}$$

The 0.1 eV for this hydride abstraction could be supplied by KE_{CM}.

The main reaction product abundance results are presented in Tables 2 and 3 and representative mass spectra are shown in Figs. 1–3. The abundances (A) are given relative to the intensities of the parent M^+, $I[M^+]$:$A[M^+{-}L] = \{I[M^+{-}L]/I[M^+]\} \times 100$; for $MO^+{-}L$ and $Tc_2^+{-}L$ the abundances are relative to MO^+ and Tc_2^+, respectively. Absolute ion intensities are expressed in mV, as are the scales on the spectra. As described previously [20] the local reactant pressure was not established but was maintained approximately constant, except where noted otherwise; the roughly linear pressure dependence of product yields suggested primarily bimolecular ($M^+ + R$) processes. Comparison of reactivities obtained for simultaneously ablated M^+ circumvents effects of minor variations in local reactant pressure and other experimental conditions. The typical range of $I[M^+]$ for which products were determined was 30–100 mV, although some products could be measured for $I[M^+]$ as low as 5 mV; some $I[MO^+{-}L]$ were measured for $I[MO^+]$ down to ca. 1 mV. Occasionally $I[^{63}Cu^+]$ was 500 mV; this glut of Cu^+ was not problematic due to its isobaric isolation and nonreactivity. A challenge in simultaneously determining relative reactivities of multiple M^+ is to achieve conditions of target concentration, chemical speciation, irradiance, t_d, etc., where the $I[M^+]$ of interest are sufficient and reasonably comparable; this is most easily realized for transition elements which exhibit similar chemistries and ionization energies, such as those studied here (Table 1).

In contrast to the results in Tables 2 and 3, studies with R = methanol (CH_3OH) and R = perfluorophenanthrene ($C_{14}F_{24}$) indicated no reactions. Although Tc^+, Re^+ and Mo^+ are quite reactive towards C–H and C–C bond activation, they contrast with the electropositive lanthanide ions, Ln^+, which react with $C_{14}F_{24}$ to produce LnF^+ (and LnF_2^+). Apparently the M^+ ionization energies are too large to enable F atom abstraction ($M^+ + C_cF_f \rightarrow M^{2+}{-}F^- + C_cF_{f-1}$). The $M^+ \rightarrow M^{2+}$ ionization energies given in Table 1 are all significantly greater than the $Ln^+ \rightarrow$

Table 2
Product yields for $\{Cu^+/Tc^+/Re^+\}^a + R \rightarrow M^+{-}L^b$

Ion	Cu	Tc	Re
$R = C_2H_4$			
M^+	*120*	*71*	*61*
$M^+{-}C_2H_4$	($<$0.3)	NO	NO
$M^+{-}C_2H_2$	($<$0.3)	1.4	3.0
$M^+{-}\{C_2H_2\}_2$	NO	NO	0.2
$R = C_3H_6$			
M^+	*88* ≈ *80*^{c}	*33* *5*^{c}	*37* *25*^{c}
$M^+{-}C_3H_6$	4 ≈ 1^c	NO NO^c	NO NO^c
$M^+{-}C_3H_4$	≈0.1 ($<$0.1)^c	5 3^c	7 13^c
$M^+{-}C_3H_2$	NO NO^c	($<$0.1) ($<$1)^c	4 2^c
$MO^+{-}C_3H_2$	NO	NO	≈20 NO
$R = cis\text{-}2\text{-}C_4H_8$		Tc^+ $Tc_2^{+\ d}$	
M^+	≈ *100*	*35* *1.0*	*60*
$M^+{-}C_4H_8$	≈5	NO NO	NO
$M^+{-}C_4H_6$	≈0.2	6 20	1
$M^+{-}C_4H_4$	NO	6 50	5
$M^+{-}\{C_4H_4\}_2$	NO	NO NO	0.6
$R = \text{cyclo-}C_6H_{10}$			
M^+	*310*	*132*	*40*
$M^+{-}C_6H_{10}$	1.4	($<$0.2)	($<$0.1)
$M^+{-}C_6H_8$	0.5	NO	NO
$M^+{-}C_6H_6$	0.7	4.7	7
$M^+{-}C_6H_4$	($<$0.05)	0.2	3
$M^+{-}\{C_6H_6\}_2$	NO	0.8	1.0
$M^+{-}\{C_6H_6\}$	NO	($<$0.1)	0.8
$\{C_6H_4\}$			
$M^+{-}C_4H_6$	2	≈0.1	($<$0.2)
MO^+	NO	*2.5*	*1.4*
$MO^+{-}C_6H_6$	NO	40	40
$MO^+{-}C_6H_4$	NO	($<$1)	20
$R = 1,5\text{-cyclo-}C_8H_{12}$			
M^+	*92*	*38*	*35*
$M^+{-}C_8H_{12}$	21	($<$0.5)	($<$0.5)
$M^+{-}C_8H_8$	1	≈5^e	3.4
$M^+{-}C_8H_6$	0.3	≈10^e	14
$M^+{-}C_6H_6$	1.6	9	9
$M^+{-}C_6H_4$	($<$0.2)	2.4	7
$M^+{-}C_4H_6$	40	1	($\leq$1)
$M^+{-}C_4H_4$	NO	3	3
$M^+{-}C_2H_2$	0.8	2	5

[a] Simultaneously ablated M^+ from the $Cu^0{-}TcO_x{-}ReO_2$ target; some reactions of ablated $MO^+$are included.

[b] Bold italicized values are parent ion absolute intensities, $I[M^+]$ or $I[MO^+]$ in mV ($M = {}^{63}Cu$, ${}^{99}Tc$ or ${}^{187}Re$). All other values are product abundances: $A[M^+{-}L] = \{I[M^+{-}L]/I[M^+]\} \times 100$; and $A[MO^+{-}L] = \{I[MO^+{-}L]/I[MO^+]\} \times 100$. All significant products are identified, except for $Cu^+ + C_6H_{10} \rightarrow Cu^+{-}\{59\text{ Da}\}$—the ligand with an apparent mass of 59 Da was not assigned and may be due to metastable adduct decay in the flight tube. Values in parentheses are limits for undetected peaks; 'NO' denotes not observed (upper limit not evaluated); approximate values are indicated where $I[M^+]$ was especially large and/or $I[M^+{-}L]$ was minuscule.

[c] $t_d = 45$ μs; all other $t_d = 35$ μs.

[d] $Tc_2^+ + C_4H_8$ was the only reaction for which metal dimer reaction was detectable.

e The A values for ${}^{99}Tc^+{-}C_8H_6$ at 201 Da and ${}^{99}Tc^+{-}C_8H_8$ at 203 Da were uncertain due to isobaric interference from ${}^{185}ReO^+$ and ${}^{187}ReO^+$. Results absent Re^+ (from a binary $Cu^0{-}TcO_x$ target) showed $A[Tc^+{-}C_8H_8] \approx A[Tc^+{-}C_8H_6]$.

Table 3
Product yields for $\{Cu^+/Mo^+/Tc^+\}^a + R \rightarrow M^+{-}L^b$

Ion	Cu	Mo	Tc
$R = C_3H_6$[c]			
M^+	*200*	*40*	*133*
$M^+{-}C_3H_6$	1	(<0.1)	(<0.1)
$M^+{-}C_3H_4$	NO	1.3	2.3
$R =$ *cis*-2-C_4H_8			
M^+	*≈80*	*55*	*30*
$M^+{-}C_4H_8$	≈10	(<0.8)	1
$M^+{-}C_4H_6$	≈0.1	7	6
$M^+{-}C_4H_4$	NO	2	3
$MO^+{-}C_4H_4$	NO	30	(<50)
$R = C_6H_{10}$[d]			
M^+	*≈100*	*17*	*≈40*
$M^+{-}C_6H_{10}$	≈30	NO	NO
$M^+{-}C_6H_8$	≈5	NO	NO
$M^+{-}C_6H_6$	≈8	30	≈100
$M^+{-}C_6H_4$	NO	(<3)	≈5
$M^+{-}\{C_6H_6\}_2$	NO	6	≈60
$M^+{-}C_4H_6$	≈30	(<3)	(<1)
MO^+	NO	*0.9*	*4.4*
$MO^+{-}C_6H_6$	NO	≈300	340

[a] Simultaneously ablated M^+ from the $Cu^0{-}MoO_3{-}TcO_x$ target; some reactions of ablated Mo^+ are included.
[b] See footnote (b) of Table 2 (here $M = {}^{63}Cu$, ${}^{98}Mo$ or ${}^{99}Tc$).
[c] $t_d = 45$ μs; all other $t_d = 35$ μs.
[d] Reactant pressure ≈4× greater than usual.

Ln^{2+} ionization energies, which range from 11.2 eV (Pr) to 13.9 eV (Lu) [26].

In the following discussion of reactions of specific ions, the assumption is that all of the observed processes are exothermic (or nearly thermoneutral) and that relative product yields reflect the intrinsic reaction rates and ion electronic structures [20]; the bonding energies of the observed products may not be directly reflected in their relative abundances. It should also be noted that metastable decay on the timescale (100 μs) of these experiments was not assessed and the observed products may dissociate on a longer timescale. Finally, it is emphasized that only positive ion products were monitored in this work and additional significant reaction pathways may have been undetected; an example would be oxidation of alkenes to epoxides:

$$H_2C{=}CH_2 + MO^+ \rightarrow H_2COCH_2 + M^+.$$

3.1. Cu^+

In many cases the behavior of naked Cu^+ accords with its quasi-inert $d^{10}s^0$ configuration and minor chemical activity compared with the preceding first-row M^+ is exhibited [27]. A notable exception in the reactivity of Cu^+ is the remarkable propensity for Cu^+ to activate allylic C–C bonds, as in the reaction of Cu^+ with 1-hexene to form $Cu^+{-}C_3H_6$ (propene) [3].

The linear alkenes employed in the present work did not offer allylic sites for activation, and condensation to $Cu^+{-}R$ was the primary channel. This inert behavior suggests that primarily ground state Cu^+ was produced. However, both cyclohexene and 1,5-cyclooctadiene reacted with Cu^+ to produce substantial $Cu^+{-}C_4H_6$ (butadiene), via unknown reaction intermediates designated as $\{Cu^+{-}R\}^*$:

$$C_6H_{10} + Cu^+ \rightarrow \{Cu^+{-}C_6H_{10}\}^* \rightarrow Cu^+{-}C_4H_6 + C_2H_4$$

$$C_8H_{12} + Cu^+ \rightarrow \{Cu^+{-}C_8H_{12}\}^* \rightarrow Cu^+{-}C_4H_6 + C_4H_6.$$

Peake and Gross [3] observed the activation of a single allylic C–C bond in linear alkenes such as pentene and hexene. Recognizing that the promotion energy of ground state ($d^{10}s^0$) Cu^+ was probably too great to facilitate oxidative insertion into the C–C bond they

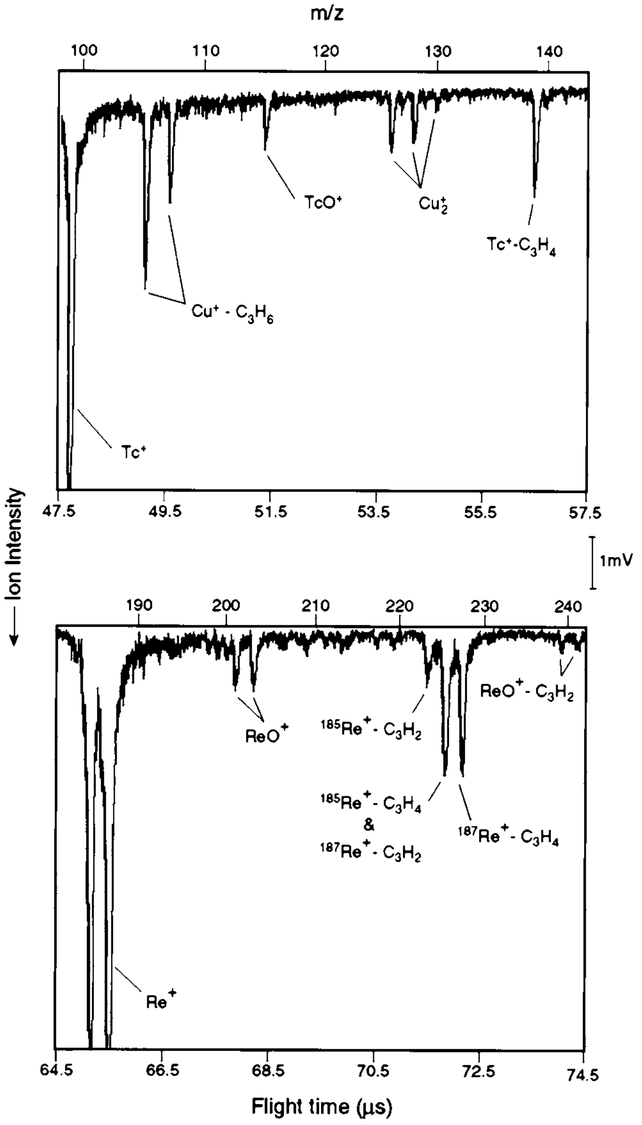

Fig. 1. Mass spectrum for $\{Cu^+/Tc^+/Re^+\} + C_3H_6$; $t_d = 35$ μs (product yields in Table 2).

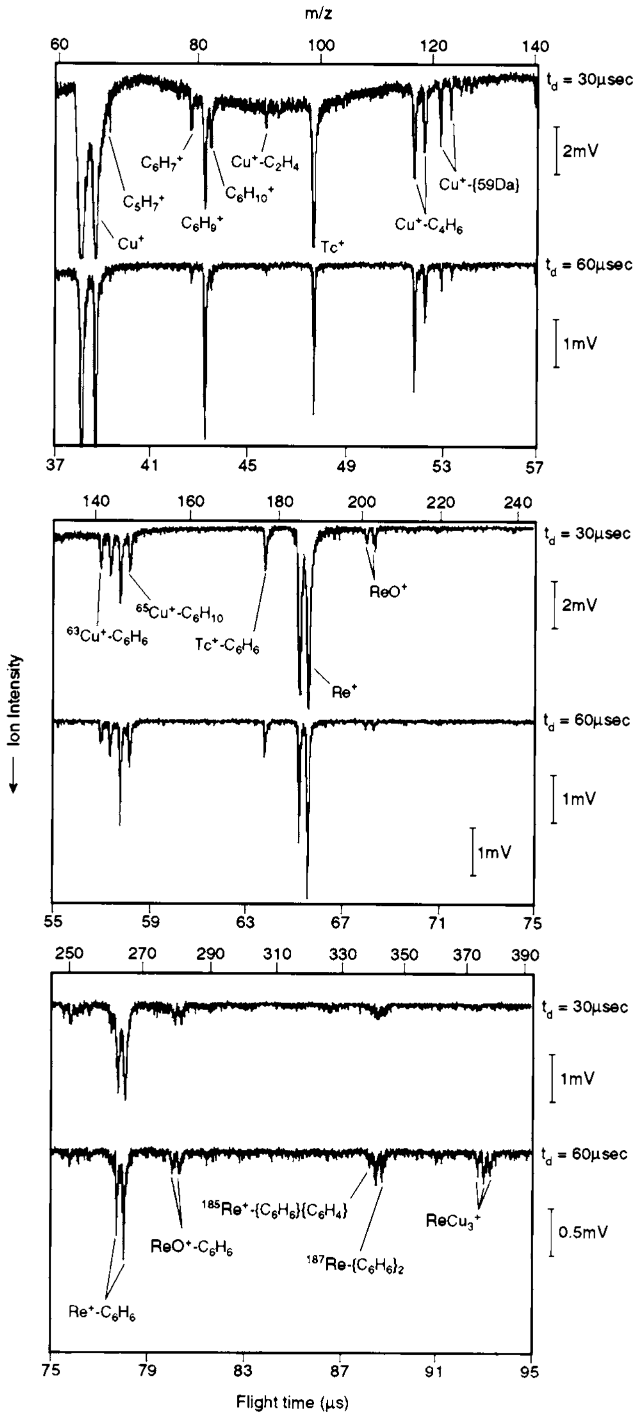

Fig. 2. Mass spectra for $\{Cu^+/Tc^+/Re^+\}$ + cyclo-C_6H_{10} for $t_d = 30$ μs and $t_d = 60$ μs.

postulated a three-centered bonded intermediate that is stabilized by the relatively high electrophilicity of Cu^+. The observation here of remarkably facile activation of both of the allylic C–C bonds in c-C_6H_{10} and 1,5–COD can be similarly rationalized by intermediates in which Cu^+ forms three-centered bonds—a schematic for a possible $\{Cu^+$–$C_6H_{10}\}^*$ intermediate is shown in Fig. 4. The ultimate Cu^+–C_4H_6 product after ethene elimination is presumed to comprise Cu^+ coordinated to both π-bonds of 1,3-butadiene. The corresponding structure for $\{Cu^+$–$C_8H_{12}\}^*$ would involve bonding of Cu^+ to carbons C3 and C7 in the 1,5-COD ring and concomitant weakening and ultimate fragmentation of the C3–C4 and C7–C8 allylic bonds.

Thermal decomposition of 1,5-COD to butadiene proceeds at 300°C [28]. The energetics of formation of 1,3-butadiene from 1,5-COD and c-C_6H_{10} are as follows [25,29]:

$$C_8H_{12} + 160\ \mathrm{kJ\ mol^{-1}} \rightarrow 2C_4H_6$$

$$C_6H_{10} + 166\ \mathrm{kJ\ mol^{-1}} \rightarrow C_4H_6 + C_2H_4\ \text{(ethene)}.$$

The ca. 160 kJ mol^{-1} endothermicity of each of these processes could be supplied by the M^+–C_4H_6 bond dissociation energy (BDE). Schwarz et al. [27] estab-

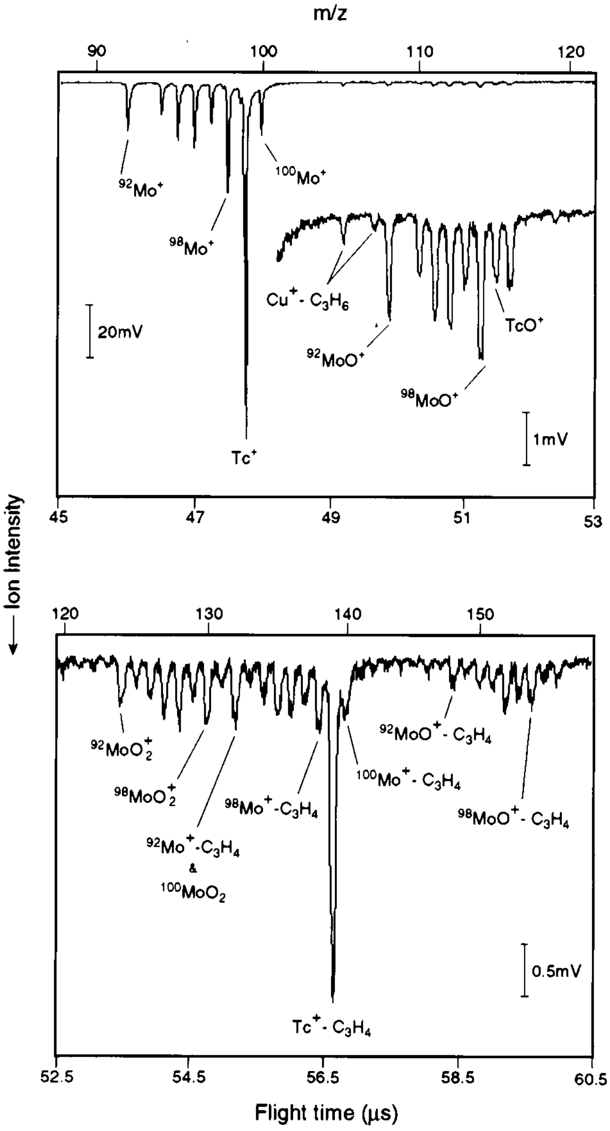

Fig. 3. Mass spectrum for $\{Cu^+/Mo^+/Tc^+\}$ + C_3H_6; $t_d = 45$ μs (product yields in Table 3).

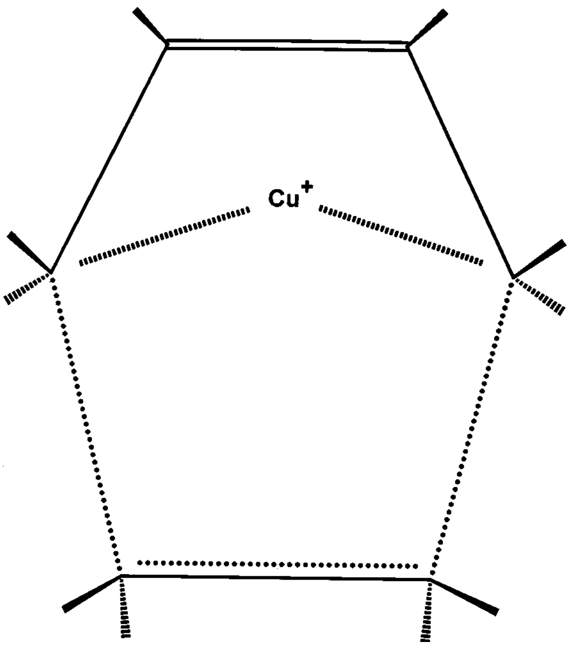

Fig. 4. Schematic of postulated intermediate for Cu^+-mediated C_2H_4-elimination from cyclohexene.

lished a lower limit of 155 kJ mol^{-1} for BDE[Cu^+–C_4H_6] which compares with BDE[Cu^+–benzene] ≈ 210 kJ mol^{-1} [30]. Incidentally, the formation of sufficiently strongly bonded Cu^+–diene complexes enables employment of volatile Cu^I–COD complexes in chemical vapor deposition processes [31].

3.2. Tc^+/Re^+

The main results are given in Table 2 and illustrated by the spectra shown in Figs. 1 and 2. The primary conclusion is that Re^+ was generally somewhat more reactive than Tc^+. This effect was manifested as greater yields for Re^+ of: (1) the dominant single H_2-loss products, e.g. $Re^+–C_2H_2 > Tc^+–C_2H_2$ from C_2H_4; (2) the minor bis-ligand products, e.g. $Re^+–\{C_2H_2\}_2 > Tc^+–\{C_2H_2\}_2$ from C_2H_4; (3) the multiple H_2-loss products, e.g. $Re^+–C_3H_2 > Tc^+–C_3H_2$ from C_3H_6 and (4) the C–C cleavage products, e.g. $Re^+–C_6H_4 > Tc^+–C_6H_4$ from C_8H_{12}. In some cases the reactivity of Re^+ was not definitively greater than that of Tc^+, e.g. $Re^+–\{C_6H_6\}_2 \approx Tc^+–\{C_6H_6\}_2$ from C_6H_{10}. An apparent anomaly was $Tc^+–C_4H_6 > Re^+–C_4H_6$ from C_4H_8; this result may reflect extremely high reactivity of the minor Tc_2^+ constituent there (see below), with emission of atomic Tc from excited adducts:

$$Tc_2^+ + C_4H_8 \rightarrow \{Tc_2^+–C_4H_6\}^* + H_2 \rightarrow Tc^+–C_4H_6 + Tc.$$

This was the only instance where sufficient Tc_2^+ was produced to possibly account for the apparent Tc^+ reactivity.

Most of the reported results were for $t_d = 35$ μs but a few experiments were carried out to assess effects of KE_I on reactivities. In Fig. 2 are shown spectra for reactions of simultaneously ablated Cu^+, Tc^+ and Re^+ with cyclohexene with the products measured for $t_d = 30$ μs and $t_d = 60$ μs; KE_I was reduced by a factor of ca. 4 by sampling with the longer delay. It is apparent that the comparative reactivities of Tc^+ and Re^+ were essentially unaffected by this difference in KE_I. That KE did not appreciably affect comparative reactivities was substantiated by the comparable relative M^+ reactivities with light R such as C_2H_4 (small KE_{CM}) and heavy R such as C_8H_{12} (large KE_{CM}).

Although the comparative reactivities of Tc^+ and Re^+ remained essentially constant regardless of t_d, some notable effects were apparent for the different $M^+ + C_6H_{10}$ reaction conditions represented by the two sets of spectra in Fig. 2. As is typical, the absolute intensity of directly ablated ions, M^+ and MO^+, decreased substantially as t_d was increased. The relative yields of reaction products such as $Cu^+–C_6H_6$ decreased relative to condensation adducts such as $Cu^+–C_6H_{10}$ with increasing t_d; presumably lower energy collision conditions reduce the probability of fragmentation of exothermically produced association products. The increased prominence of bis-ligand products such as $Re^+–\{C_6H_6\}_2$ for long t_d suggests enhanced potential for multiple $M^+–L + R$ collisions for slower ions. Finally, species attributed to coalescence in the ablation plume such as $ReCu_3^+$ increased with t_d; this effect can be attributed to the quasi-thermal nature of the ablation plume which favors aggregation processes for cooler ablated species.

The role of ion internal energy in facilitating otherwise endothermic processes can not be as directly assessed as the effects of translational energy. However, as noted above, the first excited state configuration of Tc^+ is much closer to ground state than that of Re^+ (Table 1). Accordingly, the observation of greater reactivity of Re^+ compared with Tc^+ suggests that excited Tc^{+*} did not play a dominant role in the observed reactions.

The general observation of somewhat greater reactivity of Re^+ compared with Tc^+ accords with a prevalent propensity towards enhanced reactivity upon going from the second- to third-row M^+ [17]. The effect of greater reactivity upon proceeding down a transition metal group is well-known in many aspects of inorganic chemistry, including bonding in metals and alloys, and can be rationalized in terms of the relative effectiveness of the 3d versus 4d versus 5d orbitals in chemical bonding [32]. Largely due to the lanthanide contraction, the 5d orbitals generally ex tend beyond the closed shell to a greater extent than the 4d orbitals and are accordingly more effective at overlap and concomitant bonding with valence orbitals of neighboring atoms. The comparative M^+ dehydrogenation activities are consistent with the conventional mechanism of oxidative insertion into an allylic C–H bond (–C=C–C–M^+–H) followed by relatively facile β-H abstraction ([–C=C–C=C–] . . . [H–M^+–H]) and H_2-elimination ([–C=C–C=C–] . . . $M^+ + H_2$).

3.3. Tc^+/Mo^+

Based upon the observation that W^+ is perhaps the most reactive transition metal M^+ [17], it might be predicted that Mo^+ should be the most reactive second-row M^+. However, the reactivity of Re^+ has not been sufficiently characterized to allow direct comparison with W^+, and it is feasible that Tc^+ may be as reactive as Mo^+. The primary results for simultaneous reactions of Tc^+/Mo^+ with three organic substrates are given in Table 3. The representative spectrum shown in Fig. 3 illustrates the diminished reliability of the Tc^+/Mo^+ results compared with those for corresponding Tc^+/Re^+ reactions (Fig. 1). The primary detriment with Mo^+ was the involvement of its seven important naturally occurring isotopes and their proximity to ^{99}Tc. Isobaric interferences and uncertain peak contributions were particularly problematic for minor products. As is noted in Table 3, the C_6H_{10} reactant pressure was increased substantially relative to the other reactions studied to enhance product yields and provide enhanced comparison of Tc^+ versus Mo^+ reactivities.

With C_3H_6 and C_4H_8 the dehydrogenation activity of Tc^+ was perhaps slightly greater than that of Mo^+. However, with C_6H_{10}, the yields of M^+–C_6H_6, M^+–C_6H_4 and M^+–$\{C_6H_6\}_2$ were significantly greater for Tc^+ than Mo^+. The large yields of the bis-arene products, M^+–$\{C_6H_6\}_2$, (contrast with Table 2) is attributed to the substantially greater reactant pressure. The yield of Cu^+–C_4H_6 from C_6H_{10} under these higher pressure conditions is even more remarkable than noted above.

The apparently slightly greater dehydrogenation activity of Tc^+ compared with Mo^+ might be explained by the M^+ ground electronic configurations given in Table 1. Both Mo^+ and Tc^+ exhibit ground configurations with a (highly reactive) half-filled ^{6}S 4d^5 sub-shell; the extra electron in Tc^+ occupies a 5s orbital which is empty for Mo^+. It is reasonable that this unpaired 5s electron of Tc^+ should generally enhance reactivity. The observation that the reactivity of Tc^+ is only slightly greater than that of Mo^+ suggests that the 4d orbitals play the dominant role in C–H (and C–C) activation.

3.4. MO^+ and Tc_2^+

In a few cases the MO^+ (M = Tc, Re and/or Mo) were sufficiently abundant to assess their reactivities. Each of these MO^+ was found to be substantially more effective at dehydrogenation to produce MO^+–L than were the corresponding naked M^+ at forming M^+–L; note that L is used generically and the 'L' in MO^+–L may differ from the L in M^+–L. Many condensed phase organorhenium oxide compounds have been identified [8] and the ReO^+–L produced here correspond to condensed phase X–Re^{III}O–$\{\pi$–L$\}$ (X = halogen) compounds [33]. Early (groups III and IV) transition metal MO^+ exhibit very strong M^+=O bonds which do not oxidize organic substrates [34]. Furthermore, the zero (group III) or one (group IV) free valence electrons remaining at the metal center in these MO^+ are insufficient to allow efficient oxidative insertion/activation of C–H or C–C bonds and accordingly relatively inert behavior is generally exhibited for early transition metal MO^+. Beginning at group V, two valence electrons remain at the metal center and oxidative insertion is feasible—Freiser et al. [35] demonstrated that VO^+ was essentially as effective at C–H activation as bare V^+. Some later first-row transition metals exhibit sufficiently small BDE[MO^+] (<400 kJ mol^{-1}) that oxidation processes are important; e.g. FeO^+ oxidizes methane to methanol [34]. The BDE of MoO^+ is ca. 470 kJ mol^{-1} and although not experimentally determined, the BDEs of TcO^+ and ReO^+ are probably too large (≥ 400 kJ mol^{-1}) for O-transfer to most organic substrates. In the present study, the oxidative capability of the MO^+ is not at issue since the concentration of MO^+ compared with M^+ was invariably too small to account for observed M^+–L products, and neutral alkene oxidation products (e.g. epoxides) could not be monitored. However, the intrinsic chemistries of the MO^+ were discerned by determining MO^+–L compositions and abundances, and the key observation was of highly efficient alkene dehydrogenation by MO^+.

For Tc^+=O and Re^+=O, four valence electrons remain available at the metal center and for Mo^+=O, three electrons remain available. In both cases the metal center retains an electronic configuration capable of facile C–H (or C–C) activation by oxidative insertion. The apparent enhancement in dehydrogenation efficiency by the oxo-ligand could be attributed to facilitation of β-H abstraction by coordination to the $O^{\delta-}$ ligand. An alternative scenario is C–H activation via a hydroxy intermediate (M^+=O + C–H → C–M^+–O–H) followed by β-H abstraction.

Only for the reaction $Tc_2^+ + C_4H_8$ was the minor dimer ion sufficiently abundant to assess its reactivity (Table 2). Both Tc_2^+–C_4H_6 and Tc_2^+–C_4H_4 were produced in particularly high yields, indicating a substantially greater dehydrogenation activity for Tc_2^+ compared with Tc^+. An analogous effect was established previously for the efficiency of butane dehydrogenation by the nickel group metal ions: $Ni_2^+ > Ni^+$; $Pd_2^+ > Pd^+$ and $Pt_2^+ > Pt^+$ [36]. It was determined that electronic and/or vibrational excitation of the high-energy sputtering cluster ion source employed in those experiments did not facilitate the apparently exoergic dehydrogenation processes. The ablation ion source employed here presumably produced even cooler Tc_2^+ and the high dehydrogenation activity of Tc_2^+ is taken to represent intrinsic (adiabatic) chemistry. The apparently greater efficiency of the technetium dimer at C–H bond activation can be simplistically attributed to the greater abundance of chemically active 4d orbitals; as with the MO^+, coordination of a β-H by an ancillary Tc center could further facilitate dehydrogenation.

4. Conclusions

The gas-phase organometallic chemistries of laser-ablated Tc^+, Re^+, Mo^+ and Cu^+ were compared by determining their relative alkene dehydrogenation efficiencies. As anticipated, Cu^+ was relatively inert with the condensation adduct usually the primary product. The exception was the remarkable observation of facile cracking of cyclohexene and 1,5-COD to produce abundant Cu^+–C_4H_6. This result can be rationalized by a mechanism previously invoked to explain allylic C–C activation by Cu^+. Although some cyclo-alkene cracking products were apparent for the other M^+, their abundances were minor compared with Cu^+–C_4H_6 and with their M^+–L dehydrogenation products.

In accord with general third- versus second-series transition element chemistries, Re^+ was found to be somewhat more effective at alkene dehydrogenation than Tc^+. The slightly greater activity of Tc^+ compared with Mo^+ can be rationalized in terms of the electronic configurations which furnish Tc^+ with an additional unpaired valence s-electron available for participation in C–M^+–H bonding. The present study focused on the comparative reactivities of second- (4d) versus third- (5d) row transition element ions. It should be emphasized that these M^+ are generally substantially more reactive than their first- (3d) row homologs, presumably reflecting the greater radial extension of the valence 4d/5d orbitals compared with the valence 5s/6s orbitals [32,37]. The oxide ions, TcO^+, ReO^+ and MoO^+, were each sufficiently abundant to establish that their dehydrogenation efficiencies were substantially greater than for the corresponding naked M^+—the discrepancies between M^+ and its MO^+ were greater than between different M^+. It was also found that the dehydrogenation efficiency of Tc_2^+ was considerably greater than that of Tc^+, a result in accord with previous results for other transition metal M_2^+.

In general, employing a larger reactant alkene resulted in greater complex ion abundances and more diverse reaction pathways. The disparity was particularly notable in comparing the linear versus cyclic alkenes—the latter were uniquely susceptible to C–C bond activation and resultant cracking, even with usually inert Cu^+. The results for discrepant alkenes demonstrate the versatility of this experimental approach in probing M^+ reactivities for a wide variety of metals by employing a series of appropriately reactive organic substrates.

Acknowledgements

This work was sponsored by the Division of Chemical Sciences, Office of Basic Energy Sciences, US Department of Energy, under Contract DE-AC0596OR22464 at Oak Ridge National Laboratory with Lockheed Martin Energy Research Corporation.

References

[1] K. Eller, H. Schwarz, Chem. Rev. 91 (1991) 1121.

[2] J.B. Schilling, J.L. Beauchamp, Organometallics 7 (1988) 194.

[3] D.A. Peake, M.L.J. Gross, Am. Chem. Soc. 109 (1987) 600.

[4] A.P. Sattelberger, J.C. Bryan, in: E.W. Abel, F.G.A. Stone, G. Wilkinson (Eds.), Comprehensive Organometallic Chemistry II, vol. 6, Pergamon, New York, 1995, pp. 151–166.

[5] F. Tisato, F. Refosco, B. Giuliano, Coord. Chem. Rev. 135/136 (1994) 325.

[6] C. Apostolidis, B. Kanellakopulos, R. Maier, J. Rebizant, M.L.J. Ziegler, Organometall. Chem. 411 (1991) 171.

[7] C.P. Casey, Science 259 (1993) 1552.

[8] W.A. Herrmann, F.E. Kuhn, Acc. Chem. Res. 30 (1997) 169.

[9] J.M. O'Connor, in: E.W. Abel, F.G. Stone, G. Wilkinson (Eds.), Comprehensive Organometallic Chemistry II, vol. 6, Pergamon, New York, 1995, pp. 167–229.

[10] R. Alberto, Top. Curr. Chem. 176 (1996) 150.

[11] J.K. Gibson, Radiochim. Acta 60 (1993) 121.

[12] S. Kostlmeier, V.A. Nasluzov, W.A. Herrmann, N. Rosch, Organometallics 16 (1997) 1786.

[13] B.J. Hathaway, in: G. Wilkinson (Ed.), Comprehensive Coordination Chemistry, vol. 5, Pergamon, New York, 1987, pp. 533–774.

[14] G. Van Koten, S.L. James, J.T.B.H. Jastrzebski, in: E.W. Abel, F.G.A. Stone, G. Wilkinson (Eds.), Comprehensive Organometallic Chemistry II, vol. 3, Pergamon, New York, 1995, pp. 57–133.

[15] M.W. Whitely, in: E.W. Abel, F.G.A. Stone, G. Wilkinson (Eds.), Comprehensive Organometallic Chemistry II, vol. 5, Pergamon, New York, 1995, pp. 331–391.

[16] M.J. Morris, in: E.W. Abel, F.G.A. Stone, G. Wilkinson (Eds.), Comprehensive Organometallic Chemistry II, vol. 5, Pergamon, New York, 1995, pp. 471–549.

[17] P. Mourgues, A. Ferhati, T.B. McMahon, G. Ohanessian, Organometallics 16 (1997) 210.

[18] H. Sato, Res. Chem. Intermed. 19 (1993) 67.

[19] P.B. Armentrout, R. Georgiadis, Polyhedron 7 (1988) 1573.
[20] J.K. Gibson, J. Phys. Chem., 100 (1996) 15688–15694. Organometallics, 16 (1997) 4214; J. Am. Chem. Soc. 120 (1998) 2633.
[21] C.E. Moore, Atomic Energy Levels, US National Bureau of Standards Circular 467, vols. II and III, US Government Printing Office, Washington, DC, 1971.
[22] J.K. Gibson, J. Phys. Chem. 98 (1994) 6063; 11321.
[23] P.R. Kemper, M.T. Bowers, J. Am. Soc. Mass Spec. 1 (1990) 197.
[24] F.W. McLafferty, D.B. Stauffer, The Wiley/NBS Registry of Mass Spectral Data, vol. 1, Wiley, New York, 1989, p. 17.
[25] S.G. Lias, J.E. Bartmess, J.F. Liebman, J.L. Holmes, R.D. Levin, W.G. Mallard, J. Phys. Chem. Ref. Data, 17 (Suppl. 1) (1988) pp. 40–646.
[26] W.C. Martin, L. Hagan, J. Reader, J. Sugar, J. Phys. Chem. Ref. Data 3 (1974) 771.
[27] K. Schroeter, C.A. Schalley, R. Wesendrup, D. Schroder, H. Schwarz, Organometallics 16 (1997) 986.
[28] R. Srinivasan, A.A. Levi, J. Am. Chem. Soc. 86 (1964) 3756.
[29] W. von E. Doering, M. Franck-Neumann, D. Hasselmann, R.L. Kaye, J. Am. Chem. Soc. 94 (1972) 3833.
[30] F. Meyer, F.A. Khan, P.B. Armentrout, J. Am. Chem. Soc. 117 (1995) 9740.
[31] P. Doppelt, T.H. Baum, MRS Bulletin 19 (1994) 41.
[32] J. Kouvetakis, L. Brewer, J. Phase Equilib. 14 (1993) 563.
[33] J.M. Mayer, D.L. Thorn, T.H. Tulip, J. Am. Chem. Soc. 107 (1985) 7454.
[34] D. Schroder, H. Schwarz, Angew. Chem. Int. Ed. Engl. 34 (1995) 1973.
[35] T.C. Jackson, T.J. Carlin, B.S. Freiser, J. Am. Chem. Soc. 108 (1986) 1120.
[36] T.F. Magnera, D.E. David, J. Michl, J. Am. Chem. Soc. 109 (1987) 936.
[37] J.C. Weisshaar, Acc. Chem. Res. 26 (1993) 213.